Miner Petrol (2016) 110:895–904
DOI 10.1007/s00710-016-0444-4

ORIGINAL PAPER

Batievaite-(Y), $Y_2Ca_2Ti[Si_2O_7]_2(OH)_2(H_2O)_4$, a new mineral from nepheline syenite pegmatite in the Sakharjok massif, Kola Peninsula, Russia

L. M. Lyalina [1] · A. A. Zolotarev Jr. [2] · E. A. Selivanova [1,3] · Ye. E. Savchenko [1,3] · S. V. Krivovichev [2,3] · Yu. A. Mikhailova [1] · G. I. Kadyrova [4] · D. R. Zozulya [1]

Received: 12 February 2016 / Accepted: 21 April 2016 / Published online: 4 May 2016

Abstract Batievaite-(Y), $Y_2Ca_2Ti[Si_2O_7]_2(OH)_2(H_2O)_4$, is a new mineral found in nepheline syenite pegmatite in the Sakharjok alkaline massif, Western Keivy, Kola Peninsula, Russia. The pegmatite mainly consists of nepheline, albite, alkali pyroxenes, amphiboles, biotite and zeolites. Batievaite-(Y) is a late-pegmatitic or hydrothermal mineral associated with meliphanite, fluorite, calcite, zircon, britholite-group minerals, leucophanite, gadolinite-subgroup minerals, titanite, smectites, pyrochlore-group minerals, zirkelite, cerianite-(Ce), rutile, behoite, ilmenite, apatite-group minerals, mimetite, molybdenite, and nickeline. Batievaite-(Y) is pale-cream coloured with white streak and dull, greasy or pearly luster. Its Mohs hardness is 5–5.5. No cleavage or parting was observed. The measured density is 3.45(5) g/cm^3. Batievaite-(Y) is optically biaxial positive, α 1.745(5), β 1.747(5), γ 1.752(5) (λ 589 nm), $2V_{meas.} = 60(5)°$, $2V_{calc.} = 65°$. Batievaite-(Y) is triclinic, space group P-1, a 9.4024(8), b 5.5623(5), c 7.3784(6) Å, α 89.919(2), β 101.408(2), γ 96.621(2)°, V 375.65(6) Å^3 and $Z = 1$. The eight strongest lines of the X-ray powder diffraction pattern [d(Å)(I)(hkl)] are: 2.991(100)(11-2), 7.238(36)(00-1), 3.061(30)(300), 4.350(23)(0-1-1), 9.145(17)(100), 4.042(16)(11-1), 2.819(16)(3-10), 3.745(13)(2-10). The chemical composition determined by electron probe microanalysis (EPMA) is (wt.%): Nb_2O_5 2.25, TiO_2 8.01, ZrO_2 2.72, SiO_2 29.96, Al_2O_3 0.56, Fe_2O_3 0.43, Y_2O_3 11.45, La_2O_3 0.22, Ce_2O_3 0.33, Nd_2O_3 0.02, Gd_2O_3 0.07, Dy_2O_3 0.47, Er_2O_3 1.07, Tm_2O_3 0.25, Yb_2O_3 2.81, Lu_2O_3 0.45, CaO 24.98, MnO 1.31, MgO 0.01, Na_2O 1.13, K_2O 0.02, F 2.88, Cl 0.19, H_2O 6.75 (determined on the basis of crystal structure data), O = (F,Cl) −1.25, total 97.09 wt.%. The empirical formula based on the EPMA and single-crystal structure analyses is $(Y_{0.81}Ca_{0.65}Mn_{0.15}Zr_{0.12}Yb_{0.11}Er_{0.04}Fe^{3+}_{0.04}Ce_{0.02}Dy_{0.02}Lu_{0.02}La_{0.01}Tm_{0.01})_{\Sigma 2.00}((H_2O)_{0.75}Ca_{0.70}\square_{0.55})_{\Sigma 2.00}Ca_{2.00}(\square_{0.61}Na_{0.25}(H_2O)_{0.14})_{\Sigma 1.00}(Ti_{0.76}Nb_{0.15}Zr_{0.09})_{\Sigma 1.00}[(Si_{3.91}Al_{0.09})_{\Sigma 4.00}O_{14}]((OH)_{1.56}F_{0.44})_{\Sigma 2.00}((H_2O)_{1.27}F_{0.73})_{\Sigma 2.00}$. The infrared spectrum of the mineral contains the following bands (cm^{-1}): 483, 584, 649, 800, 877, 985, 1630, 1646, 1732, 3426. Batievaite-(Y) belongs to the rosenbuschite group minerals and is the Na-deficient Y-analogue of hainite. The mineral is named in honour of the Russian geologist Iya Dmitrievna Batieva (1922–2007) in recognition of her remarkable contribution into the geology and petrology of metamorphic and alkaline complexes of the Kola Peninsula.

Editorial handling: N. V. Chukanov

✉ L. M. Lyalina
lialina@geoksc.apatity.ru

[1] Geological Institute, Kola Science Centre, Russian Academy of Sciences, Apatity, Russia

[2] Department of Crystallography, Saint-Petersburg State University, St-Petersburg, Russia

[3] Nanomaterials Research Centre, Kola Science Centre, Russian Academy of Sciences, Apatity, Russia

[4] I.V. Tananaev Institute of Chemistry and Technology of Rare Elements and Mineral Raw Materials, Kola Science Centre, Russian Academy of Sciences, Apatity, Russia

Introduction

Layered titanosilicates constitute an important group of minerals which continue to attract considerable attention of mineralogists and crystal chemists, from the viewpoint of both their mineralogy and material science (Sokolova and

Hawthorne 2013; Yakovenchuk et al. 2014; Cámara et al. 2014, 2015; Lyalina et al. 2015; Lykova et al. 2015a, b). The diversity of mineral species in this large family is due to their structural and chemical complexity, with a wide range of variations of structural modules and different cation substitution schemes. Herein, we report data on batievaite-(Y), $Y_2Ca_2Ti[Si_2O_7]_2(OH)_2(H_2O)_4$, a new mineral discovered during investigations of the rare-element mineralization of a nepheline syenite pegmatite in the Sakharjok massif, Western Keivy region, Kola Peninsula, Russia. Batievaite-(Y) is an accessory mineral formed at the late-pegmatitic or hydrothermal stage of pegmatite formation. Both the mineral and its name have been approved by the International Mineralogical Association Commission on New Minerals, Nomenclature and Classification (IMA 2015–016). Batievaite-(Y) is named in honour of the Russian geologist Iya Dmitrievna Batieva (1922–2007) in recognition of her remarkable contributions to the study of the geology and petrology of metamorphic and alkaline complexes of the Kola Peninsuila including the Sakharjok massif. The holotype specimen of batievaite-(Y) has been deposited under catalogue number GIM 7389 at the I.V. Bel'kov Museum of Geology and Mineralogy of the Geological Institute of the Kola Science Centre of the Russian Academy of Sciences (Apatity, Murmansk region, Russia).

Characterization of batievaite-(Y)

Occurrence and associated minerals

The Sakharjok massif is an alkaline intrusion, which is 8 km long and 1.5–2 km wide in its northern part. The massif is composed mainly of alkaline syenites and nepheline syenites with genetically related pegmatoid schlierens and veins (Batieva and Bel'kov 1984; Zozulya et al. 2012). Nepheline syenite hosts an economically important Zr-REE deposit in which zircon and britholite group minerals are the main ore minerals (Zozulya et al. 2012, 2015). Essexite occurring within the nepheline syenite, is a phlogopite-pyroxene-plagioclase rock with minor nepheline and amphibole. Syenite intrudes essexite resulting in the formation of numerous fractures subsequently filled by a pegmatitic material.

The studied pegmatite body occurs within the contact zone between nepheline syenite and essexite (Batieva and Bel'kov 1984) and consists of nepheline, albite, pyroxenes (including aegirine), amphiboles, biotite, analcime. Other minerals observed in pegmatite are: behoite, britholite-group minerals, calcite, cerianite-(Ce), fluorapatite, fluorite, gadolinite-subgroup minerals, ilmenite, leucophanite, meliphanite, mimetite, molybdenite, nickeline, pyrochlore-group minerals, rutile, smectite, titanite, thomsonite-Ca, zircon, and zirkelite. Batievaite-(Y) in association with hainite (Lyalina et al. 2015) occurs in aggregates of leucocratic minerals, mainly nepheline, albite and zeolite-group minerals. Batievaite-(Y) is a late-pegmatitic or hydrothermal mineral.

Morphology, physical and optical properties

Batievaite-(Y) occurs as small separate euhedral (elongated or tabular) crystals and their intergrowths (average length 0.25–0.3 mm; up to 1.6 mm in length) (Fig. 1a). Anhedral grains and their intergrowths are rare (Figs. 1b and 2). Grains of batievaite-(Y) are typically surrounded by hainite rims of 0.01–0.1 mm, rarely up to 0.15 mm thickness (Fig. 1). The hainite rim is separated from the batievaite-(Y) core by cracks filled by aggregates of different minerals, namely calcite, albite, natrolite. Batievaite-(Y) is pale-cream coloured, to almost white or very pale tan, rarely brown, with white streak and dull, greasy or, sometimes, pearly luster. The mineral is non-fluorescent in ultraviolet light. The Mohs hardness is 5–5½. No cleavage or parting was observed. The density measured by floatation in Clerici solution is 3.45(5) g/cm^3, which is in good agreement with calculated density of 3.51 g/cm^3 obtained using the empirical formula and single-crystal data. Batievaite-(Y) is optically biaxial positive, with indices of refraction α 1.745(5), β 1.747(5) and γ 1.752(5) (λ 589 nm); $2V_{meas.} = 60(5)°$ and $2V_{calc.} = 65°$. Dispersion of optical axes is moderate: r > v. The mineral is non-pleochroic. Its optical orientation is $X \sim c$. Batievaite-(Y) is insoluble in 10 % HCl. The Gladstone-Dale compatibility index ($1-K_P/K_C = -0.011$) is rated as superior (Mandarino 1981).

Infrared absorption spectroscopy

The infrared spectrum of a powdered sample of batievaite-(Y) mounted in a KBr pellet was recorded using a Nicolet 6700 FTIR (Fourier transform infrared) spectrophotometer in the range 4000–400 cm^{-1} (Fig. 3). The spectrum shows a very intense band at 3426 cm^{-1} and bands at 1646 and 1630 cm^{-1}, that can be assigned to stretching and bending vibrations of H_2O molecules, respectively (Nakamoto 2008), indicating the presence of a considerable amount of H_2O. The weak band at 1732 cm^{-1} is due to bending vibration of H_3O^+. According Chukanov (2014) and Yukhnevich (1973) the H_3O^+ bending vibration band occurs in the range of 1700–1800 cm^{-1}. The absorption bands in the 1000–800 cm^{-1} region, with two the most intense bands at 985 and 877 cm^{-1}, are assigned to Si–O stretching vibrations of the Si_2O_7 groups. Bands at 584 (weak) and 483 cm^{-1} are assigned to bending vibrations of the Si_2O_7 groups. A weak band at 649 cm^{-1} probably corresponds to Si-O-Si vibrations (Lazarev 1968).

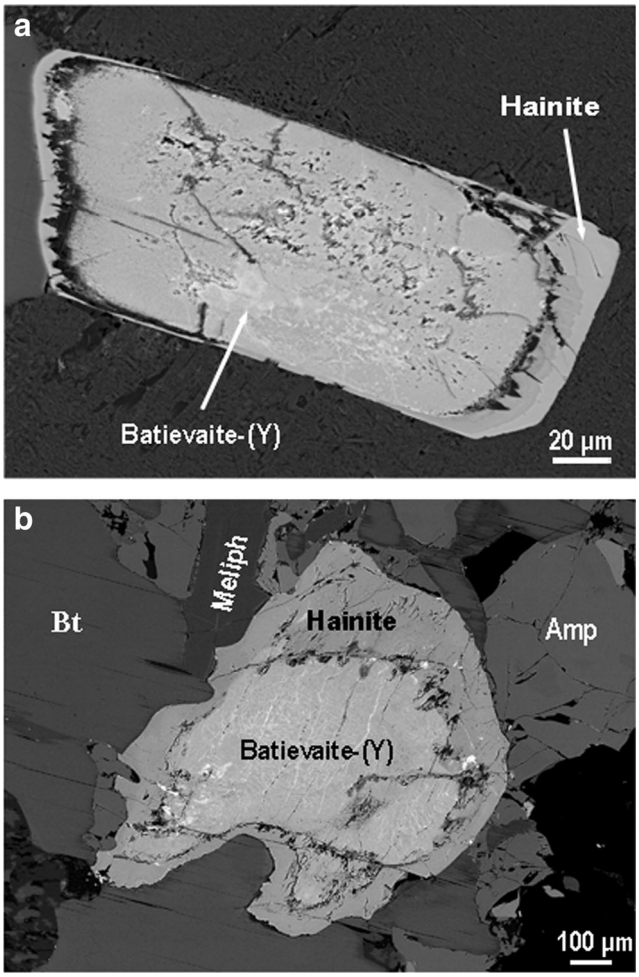

Fig. 1 Back-scattered electron images of euhedral crystals (**a**) and anhedral grains (**b**) of batievaite-(Y) surrounded by hainite rims. Amp—amphibole, Bt—biotite, Meliph—meliphanite

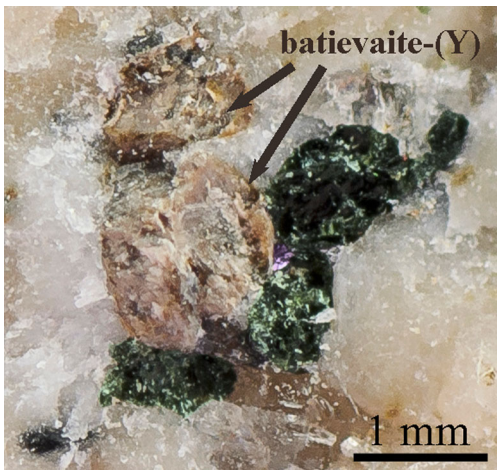

Fig. 2 Pale cream-coloured batievaite-(Y) crystals with green aegirine and violet fluorite in a zeolite aggregate

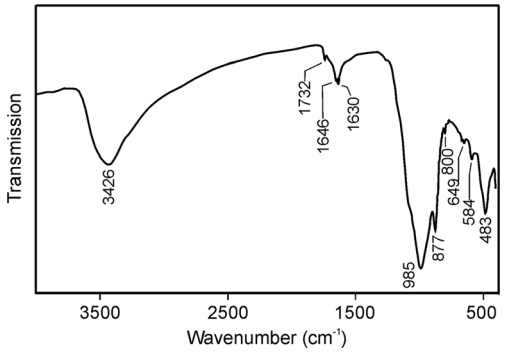

Fig. 3 Infrared spectrum of batievaite-(Y)

Chemical composition

Chemical analyses of batievaite-(Y) were carried out by means of a Cameca MS-46 electron probe microanalyzer (wavelength-dispersive spectrometry mode, 22 kV, 20–30 nA, 5–20 μm beam diameter). The following calibrant materials (and analytical lines) were used: wollastonite (Si-Kα, Ca-Kα), $Y_3Al_5O_{12}$ (Al-Kα, Y-Lα), lorenzenite (Ti-Kα, Na-Kα), $ZrSiO_4$ (Zr-Lα), Nb (Nb-Kα), $MnCO_3$ (Mn-Kα), forsterite (Mg-Kα), hematite (Fe-Kα), wadeite (K-Kα), $LaCeS_2$ (La-Lα), CeS (Ce-Lα), $LiNd(MoO_4)_2$ (Nd-Lα), GdS (Gd-Lα), $Dy_3Al_5O_{12}$ (Dy-Lα), $ErPO_4$ (Er-Lα), $Tm_3Al_5O_{12}$ (Tm-Lα), $Yb_3Al_5O_{12}$ (Yb-Lα), $Y_{2.8}Lu_{0.2}Al_5O_{12}$ (Lu-Lα), atacamite (Cl-Kα). The fluorine content was determined using a LEO-1450 Scanning Electron Microscope equipped with an XFlash-5010 Bruker Nano GmbH energy dispersive spectrometer. The electron microscope was operated at an acceleration voltage of 20 kV, and beam current of 0.5 nA, for an accumulation time of 200 s. Standard-free analysis by the P/B–ZAF method of the QuanTax system was used for the analysis of F. We did not have material sufficient for direct determination of H_2O, but the presence of H_2O was confirmed by FTIR spectroscopy and crystal structure analysis. The chemical composition of three different crystals is given in Table 1. The empirical formula based on average of the EPMA data allotted in accord with the structure (see below) is: $(Y_{0.81}Ca_{0.65}Yb_{0.11}Er_{0.04}Ce_{0.02}Dy_{0.02}Lu_{0.02}La_{0.01}Tm_{0.01}Mn_{0.15}Zr_{0.12}Fe^{3+}_{0.04})_{\Sigma 2.00}((H_2O)_{0.75}Ca_{0.70}\square_{0.55})_{\Sigma 2.00}Ca2.00(\square_{0.61}Na_{0.25}(H_2O)_{0.14})_{\Sigma 1.00}(Ti_{0.76}Nb_{0.15}Zr_{0.09})_{\Sigma 1.00}[(Si_{3.91}Al_{0.09})_{\Sigma 4.00}O_{14}](OH)_{1.56}F_{0.44})_{\Sigma 2.00}((H_2O)_{1.27}F_{0.73})_{\Sigma 2.00}$. The chondrite-normalized REE pattern for batievaite-(Y) (Fig. 4) has negative slope for LREE and positive slope for HREE with Nd, Sm, Eu below detection limit and a positive Y anomaly that is similar to associated hainite (Lyalina et al. 2015).

X-ray crystallography and crystal structure

The X-ray powder diffraction pattern for batievaite-(Y) was recorded using a Rigaku R-AXIS RAPID II diffractometer

Table 1 Chemical composition of batievaite-(Y) from the Saharjok massif, Kola Peninsula, Russia

Oxide	Sample						Average
	1	2	3	4	5	6	
SiO_2	30.1	30.8	29.6	29.8	29.6	29. 8	30.0
Al_2O_3	0.38	0.40	0.65	0.66	0.65	0.62	0.56
TiO_2	6.77	6.91	8.35	8.36	8.72	8.96	8.01
ZrO_2	3.89	4.18	2.07	1.63	1.89	2.67	2.72
Nb_2O_5	2.98	2.97	1.89	1.93	1.85	1.86	2.25
MnO	1.75	1.64	0.94	1.08	0.99	1.49	1.31
MgO	0.00	0.00	0.06	0.00	0.00	0.00	0.01
Fe_2O_3	0.53	0.48	0.53	0.53	0.31	0.22	0.43
CaO	23.9	25.9	26.0	24.4	25.1	24.6	25.0
Na_2O	0.77	0.59	1.47	1.02	1.63	1.30	1.13
K_2O	0.00	0.00	0.05	0.00	0.04	0.05	0.02
Y_2O_3	10.6	10.6	11.8	11.5	12.2	12.0	11.4
La_2O_3	0.19	0.00	0.30	0.33	0.27	0.24	0.22
Ce_2O_3	0.29	0.27	0.23	0.44	0.43	0.36	0.33
Nd_2O_3	0.00	0.00	0.00	0.11	0.00	0.00	0.02
Gd_2O_3	0.12	0.15	0.00	0.00	0.00	0.15	0.07
Dy_2O_3	0.60	0.65	0.39	0.52	0.37	0.29	0.47
Er_2O_3	1.35	1.42	0.84	0.99	0.86	0.94	1.07
Tm_2O_3	0.30	0.39	0.18	0.27	0.17	0.21	0.25
Yb_2O_3	3.51	3.60	2.58	2.37	2.44	2.37	2.81
Lu_2O_3	0.58	0.71	0.23	0.46	0.32	0.43	0.45
F	3.96	2.58	3.89	1.98	2.57	2.28	2.88
Cl	0.15	0.04	0.21	0.20	0.35	0.17	0.19
H_2O[a]	6.41	7.31	5.96	7.02	6.75	7.03	6.75
$-O=F_2,Cl_2$	1.70	1.10	1.69	0.87	1.16	1.00	1.25
Total	97.4	100.5	96.5	94.7	96.4	97.0	97.1
apfu on the basis Si + Al = 4							
Si	3.94	3.94	3.90	3.90	3.90	3.90	3.91
Al	0.06	0.06	0.10	0.10	0.10	0.10	0.09
Ti	0.67	0.66	0.83	0.82	0.86	0.88	0.79
Zr	0.25	0.26	0.13	0.10	0.12	0.17	0.17
Nb	0.18	0.17	0.11	0.11	0.11	0.11	0.13
Mn	0.19	0.18	0.10	0.12	0.11	0.17	0.15
Mg	0.00	0.00	0.01	0.00	0.00	0.00	0.00
Fe	0.05	0.05	0.05	0.05	0.03	0.02	0.04
Ca	3.35	3.55	3.66	3.42	3.54	3.46	3.49
Na	0.20	0.14	0.38	0.26	0.42	0.33	0.29
K	0.00	0.00	0.01	0.00	0.01	0.01	0.00
Y	0.74	0.72	0.82	0.80	0.85	0.84	0.80
La	0.01	0.00	0.01	0.02	0.01	0.01	0.01
Ce	0.01	0.01	0.01	0.02	0.02	0.02	0.02
Nd	0.00	0.00	0.00	0.01	0.00	0.00	0.00
Gd	0.00	0.01	0.00	0.00	0.00	0.01	0.00
Dy	0.03	0.03	0.02	0.02	0.02	0.01	0.02
Er	0.06	0.06	0.03	0.04	0.04	0.04	0.04
Tm	0.01	0.02	0.01	0.01	0.01	0.01	0.01
Yb	0.14	0.14	0.10	0.09	0.10	0.09	0.11
Lu	0.02	0.03	0.01	0.02	0.01	0.02	0.02
F	1.64	1.04	1.62	0.82	1.07	0.95	1.19
Cl	0.03	0.01	0.05	0.04	0.08	0.04	0.04
H[a]	5.60	6.23	5.23	6.14	5.93	6.15	5.88

[a] Calculated on the basis of crystal-structure study

equipped with cylindrical image plate detector using Debye-Scherrer geometry (Co$K\alpha$ radiation, d = 127.4 mm). The powder X-ray diffraction data are given in Table 2. The unit-cell parameters refined by means of the UnitCell program (Holland and Redfern 1997) are as follows: P-1, a 9.431(8), b 5.556(4), c 7.375(5) Å, α 90.10(4), β 101.44(8), γ 96.60(6) °, V 376.4(3) Å^3 that is in good agreement with crystal-structure data.

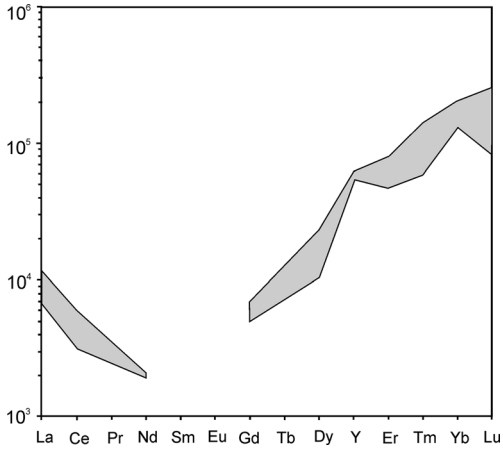

Fig. 4 Chondrite-normalised REE pattern for batievaite-(Y). For normalization factors see Sun and McDonough (1989)

The data for the crystal-structure determination of batievaite-(Y) were collected on a Bruker DUO CCD diffractometer operated at 45 kV and 0.65 mA (microfocus source) using monochromatic Mo$K\alpha$ X-radiation, frame widths of 0.5° in ω and 10 s counting time for each frame. The unit-cell parameters were refined on the basis of 5115 unique reflections (Table 3). The intensity data were reduced and corrected for Lorentz, polarization, and background effects using the Bruker software APEX2 (Bruker-AXS 2014). A semi-empirical absorption-correction based upon the intensities of equivalent reflections was applied (SADABS, Sheldrick 2008). The structure was solved with the ShelXS program using direct methods and refined with the ShelXL refinement package using standard least-squares minimization procedure (Sheldrick 2008). Occupancies of the cation positions were calculated from the experimental site-scattering factors, taking into account cation coordination parameters and empirical chemical composition. Data collection and refinement details are given in Table 3. The final coordinates, isotropic displacement parameters, refined site-scattering values and assigned populations for selected sites are listed in Table 4 (site nomenclature follows Christiansen et al. (2003)), anisotropic-displacement parameters are given in Table 5 and selected interatomic distances are reported in Table 6.

The crystal structure of batievaite-(Y) is similar to the structures of hainite and götzenite (Atencio et al. 1999; Bulakh and Kapustin 1973; Cannillo et al. 1972; Johan and Čech 1989), which belong to the rosenbuschite group (Christiansen et al. 2003). The crystal structures of minerals of this group are based upon *HOH* blocks (Fig. 5): the *H*-layer is a heteropolyhedral layer composed of $M1O_n$ and $M3O_n$ polyhedra ($n = 6–8$) linked to Si_2O_7 groups. The *O*-layer is an octahedral layer containing the M2, M4, M5 cation sites.

Table 2 X-ray powder diffraction data for batievaite-(Y) from the Saharjok massif, Kola Peninsula, Russia

I_{rel}	d_{obs}	d_{calc}	*hkl*	$I_{rel\ calc}$[a]
17	9.145	9.154	1 0 0	44
36	7.238	7.225	0 0 -1	12
23	4.350	4.342	0 -1 -1	9
16	4.042	4.038	1 1 -1	17
13	3.745	3.740	2 -1 0	16
11	3.544	3.542	2 -1 -1	12
30	3.061	3.051	3 0 0	67
100	2.991	2.992	1 1 -2	100
16	2.819	2.808	3 -1 0	31
12	2.760	2.759	0 -2 0	16
5	2.732	2.728	1 -2 0	15
10	2.595	2.594	2 0 2	6
5	2.548	2.551	3 1 0	20
5	2.143	2.143	2 -2 -2	7
3	2.013	2.019	1 2 2	17
3	1.929	1.929	3 1 2	20
3	1.843	1.844	1 0 -4	25
5	1.821	1.820	3 2 -2	15

[a] Intensity calculated from the structure

Table 3 Crystal structure data and refinement parameters for batievaite-(Y) from the Saharjok massif, Kola Peninsula, Russia

Temperature/K	293(2)
Crystal system	Triclinic
Space group	*P*-1
a (Å)	9.4024(8)
b (Å)	5.5623(5)
c (Å)	7.3784(6)
α (°)	89.919(2)
β (°)	101.408(2)
γ (°)	96.621(2)
V (Å^3)	375.65(6)
Z	1
ρ_{calc} (mg/mm^3)	3.357
μ (mm^{-1})	8.515
F(000)	368.0
Crystal size (mm)	0.19 × 0.15 × 0.09
2Θ range (°)	6.44–86.32
Index ranges	$-17 \le h \le 18$, $-10 \le k \le 9$, $-13 \le l \le 11$
Reflections collected	15,549
Independent reflections	5115[R(int) = 0.0425]
Data/restraints/parameters	5115/0/144
Goodness-of-fit on F^2	1.037
Final R indexes [$I > 2\sigma(I)$]	$R_1 = 0.0577$, $wR_2 = 0.1270$
Final R indexes [all data]	$R_1 = 0.1087$, $wR_2 = 0.1439$
Largest diff. peak/hole (e Å^{-3})	3.18/−1.66

Table 4 Atomic coordinates, site-scattering values, occupancies and equivalent isotropic displacement parameters U_{eq} (Å^2) for batievaite-(Y) from the Sakharjok massif, Kola Peninsula, Russia

Atom	s.s. (e.p.f.u)	*x*	*y*	*z*	Site occupancy	calc. s.s.[a] (e.p.f.u)	U_{eq}
M1	35.31	0.38786(5)	0.74129(6)	0.09520(5)	$Y_{0.40}Ca_{0.32}REE_{0.12}Mn_{0.08}Zr_{0.06}$ $Fe^{3+}{}_{0.02}$	33.72	0.0156(1)
M2	10.04	0.0006(2)	0.5030(3)	0.7480(2)	$(H_2O)_{0.38}Ca_{0.35}\square_{0.27}$	10.04	0.0279(5)
M3	22.2	0.38387(8)	0.7339(1)	0.59660(8)	Ca[b]	20.00	0.0179(2)
M4	3.87	0	0	½	$\square_{0.61}Na_{0.25}(H_2O)_{0.14}$	3.87	0.035(3)
M5	28.6	0	0	0	$Ti_{0.76}Nb_{0.15}Zr_{0.09}$	26.47	0.0208(2)
Si1		0.2799(1)	0.2197(2)	0.3500(1)	Si		0.0150(2)
Si2		0.2740(1)	0.2187(2)	0.7829(1)	Si		0.0151(2)
O1		0.2434(4)	0.2197(8)	0.5581(4)	O		0.0401(9)
O2		0.3791(3)	0.0037(5)	0.3353(4)	O		0.0220(5)
O3		0.3764(3)	0.0076(5)	0.8522(4)	O		0.0231(5)
O4		0.3753(3)	0.4752(5)	0.3319(4)	O		0.0227(5)
O5		0.3684(4)	0.4718(5)	0.8539(4)	O		0.0275(6)
O6		0.1222(3)	0.1882(6)	0.2130(4)	O		0.0296(7)
O7		0.1154(3)	0.1782(6)	0.8341(4)	O		0.0299(7)
X8		0.1298(4)	−0.2748(8)	0.0326(5)	$OH_{0.78}F_{0.22}$		0.0300(7)
X9		0.1197(4)	0.6987(8)	0.5279(7)	$(H_2O)_{0.64}F_{0.36}$		0.048(1)

[a] *s.s.* site scattering, *calc. s.s.* calculated site scattering for M1–M5 positions

[b] Contains a very small amount of *REE*

Details on the distribution of cations over the M1, M2, M3, M4, M5 sites in minerals of the rosenbuschite group were discussed by Christiansen et al. (2003).

The structure of batievaite-(Y) differs from that of hainite in the composition of the *O*-layer formed by the M2, M4 and M5 sites (Table 7). In batievaite-(Y), M4 is predominantly vacant, with only 39 % total occupancy by Na and H_2O molecules (Fig. 6a). The crystal structure of batievaite-(Y) contains two mixed anion positions (Table 4): X8—(OH, F) and X9—(H_2O, F) (in hainite, there are one F and one half-mixed (O, F) positions). It is noteworthy that the cation (M2, M4) and anion (X9) positions in the structure are partially occupied by H_2O molecules, which is possible because of the vacancies present in the *O*-layers.

Calculation of occupancies of the mixed H_2O-cation sites (M2, M4) was based upon the chemical analyses and structure

Table 5 Anisotropic displacement parameters (Å^2) for batievaite-(Y) from the Sakharjok massif, Kola Peninsula, Russia

Atom	U_{11}	U_{22}	U_{33}	U_{23}	U_{13}	U_{12}
M1	0.0250(2)	0.01287(15)	0.00837(14)	0.00032(9)	0.00498(11)	−0.00306(12)
M2	0.0358(10)	0.0226(7)	0.0275(8)	0.0024(5)	0.0086(6)	0.0088(6)
M3	0.0250(3)	0.0180(3)	0.0103(2)	0.00055(17)	0.00528(19)	−0.0020(2)
M4	0.025(4)	0.059(6)	0.019(3)	−0.008(3)	0.002(2)	−0.005(3)
M5	0.0203(4)	0.0292(4)	0.0096(3)	−0.0014(2)	0.0042(2)	−0.0124(3)
Si1	0.0180(5)	0.0165(4)	0.0098(4)	0.0003(3)	0.0027(3)	−0.0004(3)
Si2	0.179(5)	0.0171(4)	0.0106(4)	0.0013(3)	0.0051(3)	−0.0006(3)
O1	0.044(2)	0.068(3)	0.0098(11)	0.0037(13)	0.0089(12)	0.0036(18)
O2	0.0259(14)	0.0196(12)	0.0210(12)	−0.001(9)	0.0056(10)	0.0029(10)
O3	0.0263(14)	0.0204(12)	0.0231(12)	0.0052(9)	0.0051(10)	0.0044(10)
O4	0.0282(15)	0.0165(11)	0.0239(13)	−0.0012(9)	0.0088(10)	−0.0022(10)
O5	0.0391(18)	0.0180(12)	0.0226(13)	0.0012(10)	0.0050(11)	−0.0069(12)
O6	0.0243(15)	0.0375(17)	0.0221(13)	−0.0082(12)	−0.0054(10)	0.0000(12)
O7	0.0224(15)	0.0399(18)	0.0311(15)	0.0127(13)	0.0152(11)	0.0020(13)
X8	0.0221(15)	0.0408(18)	0.0270(15)	0.0022(12)	0.0045(11)	0.0044(13)
X9	0.0271(19)	0.048(2)	0.064(3)	−0.0003(20)	0.0053(18)	−0.0058(17)

Table 6 Selected bond lengths (Å) in the crystal structure of batievaite-(Y) from the Saharjok massif, Kola Peninsula, Russia

M1-O2	2.317(3)	M3-O1	2.998(5)	M5-O6	1.975(3)
M1-O3	2.318(3)	M3-O2	2.482(3)	M5-O6	1.975(3)
M1-O3	2.442(3)	M3-O2	2.438(3)	M5-O7	1.983(3)
M1-O4	2.300(3)	M3-O3	2.442(3)	M5-O7	1.983(3)
M1-O5	2.295(3)	M3-O4	2.411(3)	M5-X8	2.049(4)
M1-O5	2.661(4)	M3-O4	2.625(3)	M5-X8	2.049(4)
M1-X8	2.370(4)	M3-O5	2.409(3)	<M5-O,X>	2.002
<M1-O,X>	2.386	M3-X9	2.420(4)		
		<M3-O,X>	2.528	Si1-O1	1.638(3)
M2-O6	2.226(4)			Si1-O2	1.620(3)
M2-O7	2.238(4)	M4-O1	2.425(4)	Si1-O4	1.611(3)
M2-X8	2.463(4)	M4-O1	2.425(4)	Si1-O6	1.612(3)
M2-X8	2.481(4)	M4-O6	2.753(4)	<Si1-O>	1.620
M2-X9	2.347(5)	M4-O6	2.753(4)		
M2-X9	2.342(6)	M4-O7	2.634(3)	Si2-O1	1.626(3)
<M2-O,X>	2.349	M4-O7	2.634(3)	Si2-O3	1.622(3)
		M4-X9	2.112(5)	Si2-O5	1.605(3)
		M4-X9	2.112(5)	Si2-O7	1.601(3)
		<M4-O,X>	2.481	<Si2-O>	1.613

refinement and was generally similar to the calculation of site populations for mosandrite (Sokolova and Hawthorne 2013). The refined site scattering at the M2 position equals 10.04 e.p.f.u. (electron per formula unit). By analogy with mosandrite, we assign Ca remaining after the M1 and M3 sites to this site: 0.35 a.p.f.u. (atom per formula unit) = 7 e.p.f.u. The remaining site scattering 10.04 − 7 = 3.04 e.p.f.u. corresponds to 0.38 H_2O a.p.f.u. Thus, the total occupancy of M2 site is $(H_2O)_{0.38}Ca_{0.35}\square_{0.27}$. At the same time, the refined site scattering at the M4 site equals 3.87 e.p.f.u. Again, by analogy with mosandrite, we assign all Na to this site: 0.25 a.p.f.u. = 2.75 e.p.f.u. The remaining site scattering 3.87 − 2.75 = 1.12 e.p.f.u. corresponds to 0.14 H_2O a.p.f.u. Therefore, the total occupancy of M4 site is $\square_{0.61}Na_{0.25}(H_2O)_{0.14}$.

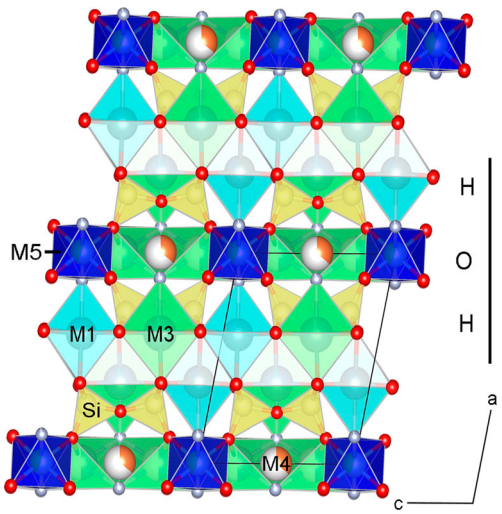

Fig. 5 The crystal structure of batievaite-(Y)

The occupancies of the mixed-anion sites X8 and X9 (Table 4) was calculated by analogy with mosandrite as well, taking into account bond-valence sums incident upon these positions (Table 8). The X8 anion site is occupied by OH groups and F (1.09 vu using cation-oxygen parameters and 0.81 vu using cation-fluorine parameters), and the X9 anion site is mainly occupied by H_2O molecules (0.65 vu using cation-oxygen parameters and 0.47 vu using cation-fluorine parameters). The presence of F in both X8 and X9 anion sites is similar to the anion site speciation in mosandrite (Sokolova and Hawthorne 2013).

The presence of hydroxyl groups in the X8 site and H_2O molecules in the X9 site results in the overall shift of the Y^{3+} and Ca^{2+} cations away from these sites in order to satisfy their bond-valence requirements by formation bonds to other anions. As a consequence, the γ angle of batievaite-(Y) changes compared to that of hainite (from ca. 101° to 96.6°, respectively), whereas the *a* and *b* parameters are shrinking (Table 7). The observed shrinkage is accompanied by considerable re-arrangement of the layer formed by the M1 and M3 polyhedra (Figs. 5 and 6b). The M1 site in batievaite-(Y) is preferentially occupied by Y^{3+} and has a sevenfold coordination, which distinguishes it from the octahedral (sixfold) coordination of the M1 site in hainite which is dominantly occupied by Ca. These changes are associated with a change in the coordination of the M3 site, which, in hainite, has a coordination number 6 or 7 and is fully occupied by Ca. In the case of batievaite-(Y), the coordination number of the M3 site is increased to 7 and 8. Therefore, the crystal structure of batievaite-(Y) can be considered as consisting of two basic blocks (Fig. 5): Na-deficient *O*-layers (Fig. 6a), typical for such TS-block minerals as mosandrite (Bellezza et al. 2009; Sokolova and Hawthorne 2013) and delindeite (Sokolova and Cámara 2007) and layers of M1–M3 polyhedra (Fig. 6b), similar to the layers of Ca polyhedra in tobermorite (Merlino et al. 1999), rinkite (Cámara et al. 2011), mosandrite (Bellezza et al. 2009; Sokolova and Hawthorne 2013) and dovyrenite (Kadiyski et al. 2008). The M1–M3 polyhedral layer is surrounded by Si_2O_7 groups thus forming *H* layer (Fig. 6c).

The empirical formula based on both chemical and single-crystal study is: $(Y_{0.80}Ca_{0.64}REE_{0.24}Mn_{0.16}Zr_{0.12}Fe^{3+}_{0.04})_{\sum 2.00}((H_2O)_{0.76}Ca_{0.70}\square_{0.54})_{\sum 2.00}Ca_{2.00}(\square_{0.61}Na_{0.25}(H2O)_{0.14})_{\sum 1.00}(Ti_{0.76}Nb_{0.15}Zr_{0.09})_{\sum 1.00}[Si_{4.00}O_{14}]((OH)_{1.56}F0.44)_{\sum 2.00}((H_2O)_{1.28}F_{0.72})_{\sum 2.00}$. The formula insignificantly differs from those obtained from chemical study. This can be explained by the presence of vacancies and H_2O in mineral.

Table 7 Ideal structural formulae and unit-cell parameters for rosenbuschite-like minerals

Mineral	Ideal structural formula						*a*, Å	*b*, Å	*c*, Å	α, °	β, °	γ, °	Sp. gr.	Z
[a]	$2A^{P}\ 2M^{H}$	$4M^{O}$			$2X^{O}{}_{M}$	$2X^{O}{}_{A}$								
[b]	M3 M1	M4 M2	M5	$(Si_2O_7)_n$	X8	X9								
Mosandrite	(Ca_3REE)	$[(H_2O)_2Ca_{0.5}\square_{0.5}]$	Ti	$(Si_2O_7)_2$	$(OH)_2$	$(H_2O)_2$	7.4222	5.6178	18.7232		101.423		$P2_1/c$	2
Rinkite	(Ca_3REE)	Na(NaCa)	Ti	$(Si_2O_7)_2$	(OF)	F_2	7.4328	5.6595	18.818		101.353		$P2_1/c$	2
Nacareniobsite-(Ce)	(Ca_3REE)	Na_3	Nb	$(Si_2O_7)_2$	(OF)	F_2	7.468	5.689	18.891		101.37		$P2_1/c$	2
Seidozerite	Na_2Zr_2	Na_2Mn	Ti	$(Si_2O_7)_2$	O_2	F_2	5.5558	7.0752	18.406		102.713		$P2/c$	2
Grenmarite	Na_2Zr_2	Na_2Mn	Zr	$(Si_2O_7)_2$	O_2	F_2	5.608	7.139	18.575		102.60		$P2/c$	2
Rosenbuschite	$Ca_4Ca_2Zr_2$	Na_2Na_4	TiZr	$(Si_2O_7)_4$	O_2F_2	F_4	10.137	11.398	7.2717	90.216	100.308	111.868	P-1	1
Kochite	Ca_2MnZr	Na_3	Ti	$(Si_2O_7)_2$	OF	F_2	10.032	11.333	7.202	90.192	100.334	111.551	P-1	2
Gotzenite	Ca_2Ca_2	$NaCa_2$	Ti	$(Si_2O_7)_2$	(OF)	F_2	9.6192	5.7249	7.3307	89.981	101.132	100.639	P-1	1
Hainite	$[Ca_3(Y,REE)]$	Na(NaCa)	Ti	$(Si_2O_7)_2$	(OF)	F_2	9.6079	5.7135	7.3198	89.916	101.077	100.828	P-1	1
Fogoite-(Y)	Ca_2Y_2	Na_3	Ti	$(Si_2O_7)_2$	(OF)	F_2	9.575	5.685	7.279	89.985	100.933	101.300	P-1	1
Batievaite-(Y)	Ca_2Y_2	$[\square_{1.0}(H_2O)_2]$	Ti	$(Si_2O_7)_2$	$(OH)_2$	$(H_2O)_2$	9.4024	5.5623	7.3784	89.919	101.408	96.621	P-1	1

Data are given according to Sokolova and Hawthorne (2013) and Cámara et al. (2015)

[a] Site nomenclature according to Sokolova (2006): M^{H} = cations of the H sheet; M^{O} = cations of the O sheet; A^{P} = cations at the peripheral (P) sites, $2X^{O}{}_{M} + 2X^{O}{}_{A}$ = anions of the O sheet not shared with Si_2O_7 groups

[b] Site nomenclature according to Christiansen et al. (2003)

Discussion

Batievaite-(Y) $Y_2Ca_2Ti[Si_2O_7]_2(OH)_2(H_2O)_4$ can be considered as a Na-deficient Y-analogue of hainite, $Na_2Ca_4(Y, REE)Ti[Si_2O_7]_2OF_3$ (Zolotarev et al. 2014), or a cation-deficient analogue of fogoite-(Y), $Na_3Ca_2Y_2Ti(Si_2O_7)_2OF_3$ (IMA 2014-098), a new Y-rich mineral of the rosenbuschite group recently described by Cámara et al. (2015). The ideal structural formulae and unit-cell parameters for the rosenbuschite-like minerals (TS-block minerals of Group I) are given in Table 7.

In general, the relations between batievaite-(Y) and hainite are very close to those between mosandrite and rinkite (Sokolova and Hawthorne 2013), which are characterized by exactly the same type of substitutions at the cation (M2, M4) and anion (X8, X9) sites in the *O*-layer. According to Sokolova and Hawthorne (2013), mosandrite and rinkite are related by the following substitution in the *O*-layer: $^{M}[(H_2O)_2 + \square_{0.5}] + {}^{X}[(OH)_2^{-} + (H_2O)_2] \rightarrow {}^{M}[Na^{+}{}_2 + Ca^{2+}{}_{0.5}] + {}^{X}[(OF)^{3-} + (F_2)^{2-}]$, where hereafter ^{M} – cation positions of the *O*-layer (M2, M4), ^{X} – anion positions of the *O*-layer (X8, X9). In the case of batievaite-(Y) and hainite, the substitution scheme is complicated by the additional substitution $^{M1}Y^{3+} + {}^{M}\square_{0.5} \rightarrow {}^{M1}Ca^{2+} + {}^{M}Ca_{0.5}{}^{2+}$. If the latter is used to describe the relations between fogoite-(Y) (fully cation-occupied analogue of batievaite-(Y)) and hainite, it takes the following form: $^{M1}Y^{3+} + {}^{M}Na^{+} \rightarrow {}^{M1}Ca^{2+} + {}^{M}Ca^{2+}$. The last scheme shows in the condition of lack of sodium in the mineral-forming environment charge increase in M1 site compensate by a further increase in the number of vacancies in the O-layer. Thus, the relations between batievaite-(Y) and hainite can be described by the following general substitution scheme: $^{M1}Y^{3+} + {}^{M}[(H_2O)_2 + \square_{1.0}] + {}^{X}[(OH)_2^{-} + (H_2O)_2] \rightarrow {}^{M1}Ca^{2+} + {}^{M}[Na^{+}{}_2 + Ca^{2+}] + {}^{X}[(OF)^{3-} + (F_2)^{2-}]$. It is possible to assume the existence of each of these schemes separately for the minerals of batievaite-(Y) – hainite series, as well as the existence of the REE-analogue of batievaite-(Y) under suitable conditions.

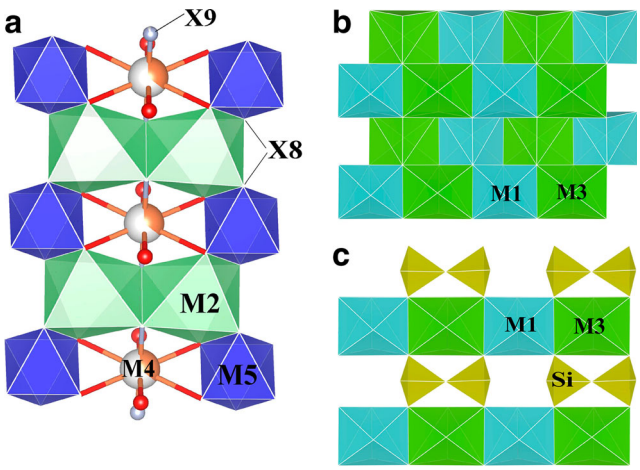

Fig. 6 The arrangement of the layers in the crystal structure of batievaite-(Y) viewed down [100]. **a** *O*-layer (M2-, M4, − and M5-centered polyhedra). **b** M1-M3 layer (M1- and M3-centered polyhedra). **c** *H*-layer (M1-, M3, − and Si-centered polyhedra)

It is worthy of note that Y-rich hainite and batievaite-(Y) from the nepheline syenite pegmatite in the Sakharjok massif are closely related paragenetically: they crystallized at the same stage of pegmatite formation and exhibit similar REE distribution. Hainite rims on batievaite-(Y) can be formed by the changes in the geochemical environment present during the crystal growth rather than the alteration processes, though the latter cannot be excluded after all. The analogy between hainite and batievaite-(Y), on one hand, and rinkite and mosandrite, on the other, may also hint that mosandrite is

Table 8 Bond-valence values[a] for batievaite-Y from the Sakharjok massif, Kola Peninsula, Russia

Atom[b]	Si1	Si2	M1 M^H	M3 A^P	M2 $M^O(3)$	M4 $M^O(2)$	M5 $M^O(1)$	Σ
O1	0.96	0.99		0.06 0.04		$0.05^{x2}\downarrow$		2.10
O2	1.01		0.39	0.28 0.25				1.93
O3		1.00	0.39 0.28	0.28				1.95
O4	1.04		0.41	0.30 0.17				1.92
O5		1.05	0.42 0.15	0.30				1.92
O6	1.03				0.17	$0.02^{x2}\downarrow$	$0.70^{x2}\downarrow$	1.92
O7		1.06			0.17	$0.03^{x2}\downarrow$	$0.68^{x2}\downarrow$	1.94
X8 (X^O_M)			0.34 [0.19]		0.09 [0.06] 0.09 [0.07]		$0.57^{x2}\downarrow$ $[0.49]^{x2}\downarrow$	1.09 [0.81]
X9 (X^O_A)				0.29 [0.21]	0.13 [0.09] 0.12 [0.09]	$0.11^{x2}\downarrow$ $[0.08]^{x2}\downarrow$		0.65 [0.47]
Total	4.04	4.10	2.38 [2.23]	1.97 [1.89]	0.77 [0.65]	0.32 [0.26]	3.90 [3.74]	

[a] Bond-valence parameters according Brese and O'Keeffe (1991)

[b] Bond-valence values calculated on the basis of following sites composition

M1 = $Y_{0.52}Ca_{0.32}Mn_{0.08}Zr_{0.06}Fe^{+3}{}_{0.02}$; M2 = Ca (35 % occupancy); M3 = Ca; M4 = Na (25 % occupancy); M5 = $Ti_{0.76}$ $Nb_{0.15}Zr_{0.09}$; values in [] calculated using cation-F parameters

not alteration product of rinkite as proposed previously by Slepnev (1957). However, more experimental evidence is needed in order to make a final conclusion on this matter.

Acknowledgments The study was supported by the Russian Foundation for Basic Research (grant No. 16-05-00427). AAZ is grateful to President Federation Grant for Young Candidates of Sciences (MK-3296.2015.5). SVK acknowledges financial support from Saint-Petersburg State University (grant # 3.38.136.2014). X-ray diffraction studies were conducted at the XRD Resource Centre of Saint-Petersburg State University. We thank reviewers Fernando Camara, Anthony Robert Kampf and Igor Pekov for their helpful comments.

References

Atencio D, Coutinho JMV, Ulbrich MNC, Vlach SRF, Rastsvetaeva RK, Pushcharovsky DY (1999) Hainite from Poços de Caldas, Minas Gerais, Brazil. Can Mineral 37:91–98

Batieva ID, Bel'kov IV (1984) The Saharjok alkaline intrusion: rocks and minerals. Kola Branch USSR Acad Sci Apatity, 133 pp [in Russian]

Bellezza M, Merlino S, Perchiazzi N (2009) Mosandrite: structural and crystal-chemical relationships with rinkite. Can Mineral 47:897–908

Brese NE, O'Keeffe M (1991) Bond-valence parameters for solids. Acta Crystallogr B47:192–197

Bruker-AXS (2014) APEX2. Version 2014.11-0. Madison, Wisconsin, USA

Bulakh AG, Kapustin YL (1973) Götzenite from alkaline rocks of Turii Peninsula (Kola Peninsula). Zap Vsesoiuznogo Mineral Obshch 102:464–466 [in Russian]

Cámara F, Sokolova E, Hawthorne FC (2011) From structural topology to chemical composition. XII. Titanium silicates: the crystal chemistry of rinkite $Na_2Ca_4REETi(Si_2O_7)_2OF_3$. Mineral Mag 75(6):2755–2774

Cámara F, Sokolova E, Abdu YA, Hawthorne FC (2014) Nafertisite, $Na_3Fe^{2+}{}_{10}Ti_2(Si_6O_{17})_2O_2(OH)_6F(H_2O)_2$, from Mt. Kukisvumchorr, Khibiny alkaline massif, Kola peninsula, Russia. Eur J Mineral 26: 689–700

Cámara F, Sokolova E, Abdu YA, Hawthorne FC, Charrier T, Dorcet V, Carpentier J-F (2015) Fogoite-(Y), IMA2014-098. CNMNC Newsletter No. 24, April 2015, page 250. Mineral Mag 79(2): 247–251

Cannillo E, Mazzi F, Rossi G (1972) Crystal structure of götzenite. Sov Phys Crystallogr 16:1026–1030

Christiansen CC, Johnsen O, Makovicky E (2003) Crystal chemistry of the rosenbuschite group. Can Mineral 41:1203–1224

Chukanov NV (2014) Infrared spectra of mineral species. Springer Verlag, Dordrecht

Holland TJB, Redfern SAT (1997) Unit cell refinement from powder diffraction data: the use of regression diagnostics. Mineral Mag 61(1):65–77

Johan Z, Čech F (1989) New data on hainite, $Na_2Ca_4[(Ti,Zr,Mn,Fe,Nb,Ta)_{1.50}\square_{0.50}](Si_2O_7)F_4$ and its crystallochemical relationship with

götzenite, $Na_2Ca_5Ti(Si_2O_7)_2F_4$. C R Acad Sci II 308:1237–1242 [in French, with extended English abstract]

Kadiyski M, Armbruster T, Galuskin EV, Pertsev NN, Zadov AE, Galuskina IO, Wrzalik R, Dzierzanowski P, Kislov EV (2008) The modular structure of dovyrenite, $Ca_6Zr[Si_2O_7]_2(OH)_4$: alternate stacking of tobermorite and rosenbuschite-like units. Am Mineral 93:456–462

Lazarev AN (1968) Kolebatel'nye Spectry I Stroenie Silikatov (Vibrational spectra and structure of silicates). Nauka, Leningrad, 347 pp [in Russian]

Lyalina LM, Zolotarev AA Jr, Selivanova EA, Savchenko YE, Zozulya DR, Krivovichev SV, Mikhailova YA (2015) Structural characterization and composition of Y-rich hainite from Sakharjok nepheline syenite pegmatite (Kola Peninsula, Russia). Miner Petrol 109:443–451

Lykova IS, Pekov IV, Zubkova NV, Chukanov NV, Yapaskurt VO, Chervonnaya NA, Zolotarev AA (2015a) Crystal chemistry of cation-exchanged forms of epistolite-group minerals, Part I. Ag- and Cu-exchanged lomonosovite and Ag-exchanged murmanite. Eur J Mineral 27:535–549

Lykova IS, Pekov IV, Zubkova NV, Yapaskurt VO, Chervonnaya NA, Zolotarev AA, Giester G (2015b) Crystal chemistry of cation-exchanged forms of epistolite-group minerals. Part II. Vigrishinite and Zn-exchanged murmanite. Eur J Mineral 27:669–682

Mandarino JA (1981) The Gladstone-Dale relationship: part IV. The compatibility concept and its application. Can Mineral 19:441–450

Merlino S, Bonaccorsi E, Armbruster T (1999) Tobermorites: their real structure and order–disorder (OD) character. Am Mineral 84:1613–1621

Nakamoto K (2008) Infrared and Raman spectra of inorganic and coordination compounds, theory and applications in inorganic chemistry. Wiley, Hoboken, Part A, 432 pp

Sheldrick GM (2008) A short history of SHELX. Acta Crystallogr A64: 112–122

Slepnev YS (1957) On the minerals of the rinkite group. Izv Akad Nauk SSSR Ser Geol 3:65–75 [in Russian]

Sokolova E (2006) From structure topology to chemical composition. I. Structural hierarchy and stereochemistry in titanium disilicate minerals. Can Mineral 44:1273–1330

Sokolova E, Cámara F (2007) From structure topology to chemical composition. II. Titanium silicates: revision of the crystal structure and chemical formula of delindeite. Can Mineral 45: 1247–1261

Sokolova E, Hawthorne FC (2013) From structure topology to chemical composition. XIV. Titanium silicates: refinement of the crystal structure and revision of the chemical formula of mosandrite, $(Ca_3REE)[(H_2O)_2Ca_{0.5}\square_{0.5}]Ti(Si_2O_7)_2(OH)_2(H_2O)_2$, a Group-I mineral from the Saga mine, Morje, Porsgrunn, Norway. Mineral Mag 77(6):2753–2771

Sun SS, McDonough WF (1989) Chemical and isotopic systematics of oceanic basalts: applications for mantle composition and processes. In: Saunders AD, Norry MJ (eds) Magmatism in the ocean basins, Special Publication of the Geological Society 42. Geological Society, London, pp 313–345

Yakovenchuk VN, Krivovichev SV, Ivanyuk GY, Pakhomovsky YA, Selivanova EA, Zhitova EA, Kalashnikova GO, Zolotarev AA, Mikhailova JA, Kadyrova GI (2014) Kihlmanite-(Ce), $Ce_2TiO_2[SiO_4](HCO_3)_2(H_2O)$, a new rare-earth mineral from the pegmatites of the Khibiny alkaline massif, Kola Peninsula, Russia. Mineral Mag 78(3):483–496

Yukhnevich GV (1973) Infrakrasnaya Spektroskopiya Vody (Infrared spectroscopy of water). Nauka, Moscow, 208 pp [in Russian]

Zolotarev A, Krivovichev S, Lyalina L, Selivanova E (2014) Crystal structure and chemistry of Na-deficient Y-dominant analogue of hainite/götzenite. 21st General Meeting of IMA. South Africa. Abstract Volume: 329

Zozulya DR, Lyalina LM, Eby N, Savchenko YE (2012) Ore geochemistry, zircon mineralogy, and genesis of the Sakharjok Y–Zr deposit, Kola Peninsula, Russia. Geol Ore Depos 54:81–98

Zozulya DR, Lyalina LM, Savchenko YE (2015) Britholite ores of the Sakharjok Zr–Y–REE deposit, Kola Peninsula: geochemistry, mineralogy, and formation stages. Geochem Int 53(10):892–902